Available online at www.sciencedirect.com

SCIENCE DIRECT®

Journal of Molecular Catalysis A: Chemical 204–205 (2003) 779–786

JOURNAL OF MOLECULAR CATALYSIS A: CHEMICAL

www.elsevier.com/locate/molcata

Bonding of NO on $Ni_xMg_{1-x}O$ powders: an EPR and computational study

Mario Chiesa [a], Maria Cristina Paganini [a], Elio Giamello [a], Cristiana Di Valentin [b], Gianfranco Pacchioni [b,*]

[a] *Dipartimento di Chimica IFM, Istituto Nazionale per la Fisica della Materia, Università di Torino, Via P. Giuria, I-10125 Torino, Italy*

[b] *Dipartimento di Scienza dei Materiali, Istituto Nazionale per la Fisica della Materia, Università di Milano–Bicocca, Via R. Cozzi 53, 20125 Milan, Italy*

Received 25 September 2002; received in revised form 24 January 2003; accepted 11 February 2003

Dedicated to Professor Renato Ugo on the occasion of his 65th birthday

Abstract

In this paper, we review the reactivity of the paramagnetic NO molecule with Ni-doped MgO based on electron paramagnetic resonance (EPR) spectra and density functional theory (DFT) cluster model calculations. The EPR spectrum of the NiO/MgO sample recorded at 77 K under NO pressure is characterized by two distinct signals, one assigned to monomeric NO physisorbed on low-coordinated Mg^{2+} ions and the other to NO adsorbed on terrace Ni^{2+} ions. The latter interaction is found to be at least three times larger than the former. The nature of NO bonding to Ni^{2+} ions is analyzed in detail. The EPR spectrum proves the presence of one unpaired electron localized on the Ni 3d shell. The DFT calculations indicate that the unpaired electron sits on the $d_{x^2-y^2}$ orbital, while the Ni^{2+} d_{z^2} electron is coupled with the NO π^*_{xz} unpaired electron, producing a NO–Ni^{2+} bond with dominant covalent character.

Keywords: Electron paramagnetic resonance; Density functional theory; Oxide surfaces; Chemisorption

1. Introduction

The bonding of gas-phase molecules with the surface of oxides has important technological implications in area like catalysis and sensors. The combination of two metals in an oxide matrix may lead to the production of materials with peculiar electronic and structural properties, suitable for new catalytic activities [1–3]. Ideal solid solutions of NiO and MgO can be obtained over the whole mole-fraction range (with $0 \leq x \leq 1$, where x is the NiO mole fraction) since the two oxides crystallize in the same rock-salt structure, present similar ionic parameters, and produce typical cubic microcrystallites [4]. The surface ions of both MgO and NiO can be five-, four- or three-fold-coordinated depending on their location, (1 0 0) faces, edges and steps, or corners, respectively. Ni ions embedded in a MgO matrix present very similar chemical properties to those of the same ions in NiO [2,3,5]. Infrared frequencies and adsorption energies of molecules adsorbed on powders [6–8] and thin films [9] of mixed NiO/MgO, compared with

* Corresponding author. Tel.: +39-02-6448-5219; fax: +39-02-6448-5400.
E-mail address: gianfranco.pacchioni@unimib.it (G. Pacchioni).

1381-1169/$ – see front matter © 2003 Elsevier B.V. All rights reserved.
doi:10.1016/S1381-1169(03)00364-9

those of pure NiO, support this conclusion. Therefore, diluted NiO/MgO systems are not only useful for the analysis of NO reactivity on MgO in the presence of growing percentage of Ni^{2+} ions, but also to study the surface chemistry of Ni^{2+} ions, as compared to that of pure NiO.

In the present work, we analyze the reactivity of NO with NiO/MgO high surface area samples by means of the electron paramagnetic resonance (EPR) technique, which cannot be applied on bare NiO, since the strong antiferromagnetic behavior of this oxide prevents the observation of surface paramagnetic species [10]. The EPR spectroscopy provides information which is complementary to that obtained with other techniques applied to NiO(1 0 0) single crystals or thin films. A great effort by various groups has been devoted to NO adsorption on these two latter systems [11–14] so that accurate data on geometry and adsorption energy are available, making NO/NiO an excellent system to test theoretical approaches. In particular, photoelectron diffraction (PD) on NiO(1 0 0) thin films has shown that the molecule is bound with a Ni–N distance of 1.88 Å and a tilt angle $\theta = 59^{\circ}$ from the surface normal [11,12]. Thermal programmed desorption (TPD) on NiO single crystals result in a desorption energy of 0.57 eV [13].

Recently, a lively debate was opened on the actual capability of theoretical methods to reproduce these results and to correctly describe the bonding of molecules, such as NO, to the NiO surface [11,15–17]. In this paper, we review old EPR experiments [10] and we present new spectra recorded at high resolution; the results are combined with those of theoretical calculations on the same system with the aim of giving a clear and accurate account of (i) the nature of the NO bonding to the Ni^{2+} ions and (ii) the reactivity of MgO with NO in the presence of Ni^{2+} impurities.

2. Experimental and computational details

2.1. Experimental

$Ni_xMg_{1-x}O$ solid solutions were prepared by decomposition of $Mg(OH)_2$ which had been impregnated with an aqueous solution of $Ni(NO_3)_2$ as reported in [4]. The impregnated $Mg(OH)_2$ was dried at 393 K. The mixture was then ground and reslurried in water in order to achieve complete mixing through the hydroxide mass. The dried, nitrate impregnated $Mg(OH)_2$ was then placed into a quartz cell attached to an EPR tube and slowly decomposed under dynamic vacuum (10^{-5} mbar) at 523 K for 16 h. The temperature of the furnace was then increased in stages up to 1173 K. The sample was kept at this temperature for 2 h in order to allow time for ionic diffusion and to obtain a homogeneous oxide solid solution. In such conditions, the surface is practically free from hydroxyl or carbonate contaminants and displays mainly cations and anions in coordination 5 (terraces) but also several families of ions in coordination 4 and 3 located at edges, kinks, corners of the high surface area samples.

We have investigated the interaction of NO with three differently loaded NiO/MgO samples (1, 5, 10 molar fraction, respectively). The BET surface areas of the solids prepared as described above range from 250 $m^2\,g^{-1}$ in the case of $Ni_{0.01}Mg_{0.99}O$ to about 100 $m^2\,g^{-1}$ for $Ni_{0.1}Mg_{0.9}O$. High purity ^{14}NO (Matheson) gas was purified before admission by the freeze-pump-thaw technique. X-band EPR spectra were recorded at 298 and 77 K on a Bruker EMX spectrometer equipped with a cylindrical cavity.

2.2. Computational aspects

This work is an extension of our recent theoretical study on the NiO/NO interaction [16]; the computational approach is the same adopted in [16] and only the main aspects of the method used are given. The Ni-doped MgO(1 0 0) surface has been modeled by a $NiMg_8O_9$ cluster (Fig. 1) embedded in ± 2 point charges (PC) to account for the Madelung field at the adsorption site [18]. In order to prevent the artificial polarization of the O^{2-} anions at the cluster borders, effective core potentials (ECPs) with no associated basis functions are added to the positive PCs around the cluster [19,20]. The cluster wave function has been constructed using the following Gaussian type basis sets: Mg and O atoms were described with the 6-31G basis set [21]; the four oxygen ions closest to the Ni impurity have been treated with a 6-31+G* basis set [21] including diffuse (+) and d polarization (*) functions; Ni has been described by a 6-31G* basis set [22]; the 6-31+G* basis set has been used on the N and O atoms of the NO molecule. Spin polarized (unrestricted) and restricted open (RO) shell calculations

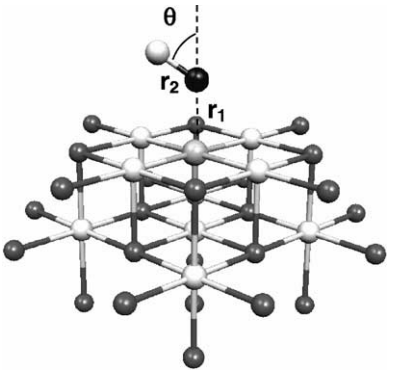

Fig. 1. $NiMg_8O_9$ cluster model of NO adsorbed on the (100) surface of Ni-doped MgO. Open circles: O; gray circles: Mg; NO is adsorbed above a Ni^{2+} cation replacing a Mg^{2+} cation.

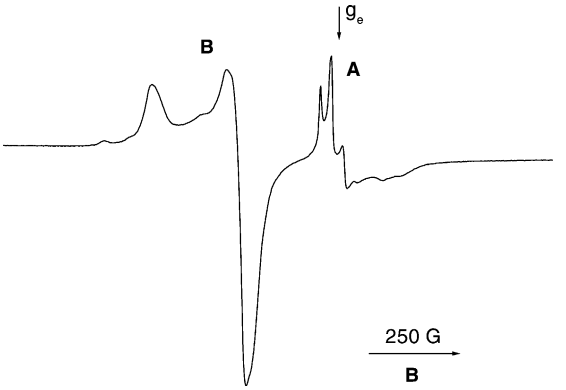

Fig. 2. EPR spectrum at 77 K of Ni/MgO (1%) solid solution under 20 Torr of NO.

were performed at the density functional theory (DFT) level using the gradient corrected B3LYP hybrid exchange-correlation functional [23,24].

Geometry optimizations were performed by means of analytical gradients with no symmetry constraints. Beside the N and O atoms of the NO molecule, also the Ni atom and the first four neighboring O atoms of the cluster were allowed to relax. The binding energies have been corrected by the basis set superposition error (BSSE) using the counter-poise correction [25]. The calculations have been performed using the Gaussian 98 program package [26].

3. Results and discussion

3.1. Experimental results

The EPR spectra of all bare activated samples are characterized by a wide band at $g \approx 2$ due to bulk Ni^{2+} ions in octahedral coordination whose intensity is directly related to the nickel loading. The right wing of this band therefore interferes with the EPR spectra of adsorbed NO in particular for higher loading samples: thus, though the results are similar on the three systems, we will discuss only spectra related to the 1% NiO/MgO sample in which the overlap between the bulk Ni^{2+} signal and that due to NO is negligible.

The EPR spectrum of NiO/MgO recorded at 77 K under a 20 Torr NO is reported in Fig. 2 and consists of two clearly separated signals. The former one, at high field (signal A) is due to monomeric NO weakly adsorbed on exposed Mg^{2+} cation sites. This spectrum has been widely discussed elsewhere [27] and is due to three species exhibiting a rhombic structure with $g_{xx} > g_{yy} \gg g_{zz}$ (spin-Hamiltonian parameters of NO (a), NO (b) and NO (c) in Table 1). The g_{xx} component is split into three lines by the hyperfine interaction with the N ($I = 1$) nucleus. A weaker coupling is also present on the z component but the structure is unresolved. The three species differ uniquely for the value of the g_{zz} component which indicates a different extent of NO interaction with the surface. A higher g_{zz} value corresponds to both a stronger (electrostatic) interaction with the site and a larger splitting of the π^* orbitals of the NO molecule. On the remaining (weaker) sites of the surface NO does not adsorb in monomeric form but gives rise to diamagnetic adsorbed dimers [27]. On the Ni-doped system the EPR features of the NO–MgO interaction are the same recorded on the bare MgO. This fact seems to indicate that the morphology of high area MgO is maintained also in the presence of non-negligible amounts of Ni^{2+} in the solid.

The second signal, on the left hand side of Fig. 2 (signal B) is an axial signal with $g_{\parallel} = 2.274$ and $g_{\perp} = 2.131$. As discussed in a previous paper [10] the spectral features of the signal are those expected for a d^9 system in axial symmetry and are unambiguously assigned to surface Ni^{2+} ions interacting with NO (signal B is observed only in the presence of Ni). This finding indicates that one of the two unpaired electrons of Ni^{2+} (d^8) couples with the unpaired electron

Table 1
Spin-Hamiltonian parameters of the paramagnetic species present in the spectrum reported in Fig. 2 [27]

Species		g_{xx}	g_{yy}	g_{zz}	Δ (eV)	A_{xx}	A_{yy}	A_{zz}
A	NO (a)	1.9948 ± 0.0005	1.9976 ± 0.0020	1.8900 ± 0.0002	0.075	32	2.57	8.86
	NO (b)	1.9948 ± 0.0005	1.9971 ± 0.0020	1.9188 ± 0.0002	0.1	32.5	Unres	Unres
	NO (c)	1.9955 ± 0.0020	1.9957 ± 0.0020	1.9610 ± 0.0002	0.2	32.6	Unres	Unres
B	Ni^+	2.131	2.131	2.274				

of NO. The interaction is reversible and upon NO evacuation both A and B signals disappear after a brief pumping off at RT and can be formed again by a new NO adsorption.

The formation and the evolution of A and B signals as a function of NO equilibrium pressure is reported in Fig. 3. The experiment covers the range between 0.1 and 40 Torr of NO pressure. NO is adsorbed at RT and each spectrum is then recorded at 77 K. Both species are visible since the early stages of the interaction and the spectral features basically remain the same along the experiment. The NO–Mg^{2+} species however is very weak in the initial stages of the interaction (0.1–4 Torr) for which the spectrum is dominated by the NO–Ni^{2+} B species which should thus have a higher binding energy than species A. This is confirmed by the spectra recorded at RT (not shown) for the same NO pressure present in Fig. 3. Here, the B signal is still present while the A signal is not observed. At the resonant field typical of A, a very weak signal is now present due to a tiny amount of NO_2^{2-} radicals irreversibly formed by NO chemisorbed on particularly basic O^{2-} sites [27]. This species was also present in the low temperature spectra of Fig. 3 but was buried in features of the much more intense species A. The fact that the NO adduct on Ni^{2+} forms at RT while the NO–Mg^{2+} species does not, indicates that the former species, though weakly bound to the surface as indicated by the reversibility to evacuation, has a binding energy with the surface higher than the second one.

A quantitative evaluation of the relative amounts of the two species monitored at various NO pressure in Fig. 3 is reported in Fig. 4. The data have been derived by double integration of the whole experimental EPR spectra (line A + B, total amount) and by a successive partial integration of the two halves of the EPR spectrum obtained cutting the line between the two A and

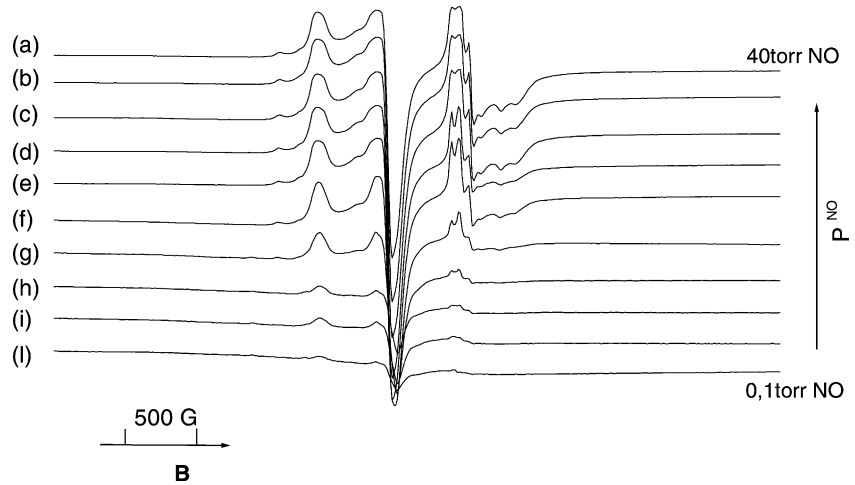

Fig. 3. EPR spectra of Ni/MgO (1%) recorded at 77 K under different NO pressures: (a) 40 Torr, (b) 30 Torr, (c) 25 Torr, (d) 20 Torr, (e) 15 Torr, (f) 10 Torr, (g) 4 Torr, (h) 1 Torr, (i) 0.5 Torr, (l) 0.1 Torr.

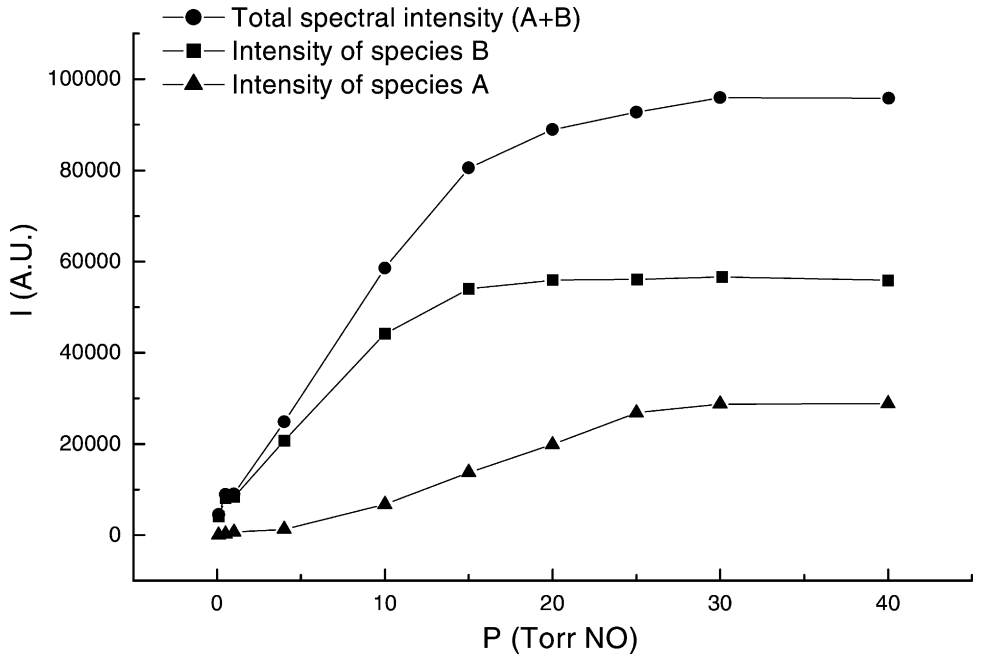

Fig. 4. Integrated intensity of the EPR spectra reported in Fig. 2 (circles). Squares are the integrated intensities of signal B, whereas triangles correspond to the integrated intensity of monomeric adsorbed NO (signal A).

B signals. Despite the intrinsic approximation of this method, it results that the NO–Ni^{2+} complex is the most abundant at low NO pressure whereas for pressures higher than 20 Torr the whole intensity becomes constant and the two A and B species are more or less in a 2:1 ratio.

This quantitative evaluation of the A/B ratio allows us to assign signal B to the NO adducts on 5-coordinated Ni^{2+} ions on the (1 0 0) terraces. This can briefly be explained as follows. In an ideal system of high surface MgO (or NiO/MgO) with about $200\,m^2\,g^{-1}$ surface area and formed by small regular cubelets, the fraction of 4- and 3-coordinated ions is about 6.6%. This fraction tends to increase while increasing the non-ideality of the microcrystals with formation of steps, kinks and similar morphological defects. It is reasonable to assume that in a real high area MgO the fraction of 3- and 4-coordinated ions should amount to about 10% of the total surface ions. Assuming (and this is not certainly the case) that all these ions are probed by NO in terms of NO–Mg^{2+} species A, the Ni^{2+} ions probed by NO in terms of species B should also be at least 10% of all the surface exposed cations. This is clearly impossible in a sample that contains 1% of Ni^{2+} ions and whose surface composition is expected to be not so different from the bulk composition. The only way to rationalize the quantitative results is to assume that about 8–10% of the total 3- and 4-coordinated Mg^{2+} ions are monitored by NO in terms of species A while *all* 5-coordinated Ni^{2+} at the flat (1 0 0) surfaces are monitored in terms of species B.

3.2. Computational results

It is clear from the experimental observations that the reactivity of NO with the MgO matrix is not affected by the presence of Ni^{2+} ions, so that we can easily refer to the results reported in [27] where it was shown that NO prevalently adsorbs on the MgO(1 0 0) terraces and prefers to form dimers ($(NO)_2$, $D_e = 0.1$ eV), while only on low-coordinated cations the interaction of NO monomers with the MgO surface ($D_e = 0.13$–0.20 eV) is such to prevent the formation of diamagnetic $(NO)_2$ species [27].

Table 2
Binding energies and geometrical parameters of the optimized structures for NO adsorbed on $NiMg_8O_9$ ($^2A''$ state) [16]

	U-B3LYP	RO-B3LYP	Experimental value
D_e (eV)	0.48	−0.03	0.57[a]
r_1(Ni–N) (Å)	1.873	1.789	1.88[b]
r_2(N–O) (Å)	1.173	1.183	1.12[b]
θ (°)	58.0	60.5	59[b]
Spin on Ni	1.63 (−0.83 on NO)	0.81	∼1[c]
$\langle\hat{S}^2\rangle$	1.36	0.75	–

[a] [13].
[b] [11,12].
[c] This work.

First, we summarize the main aspects of the interaction of NO with the Ni^{2+} species [16]. We have computed the NO/Ni–MgO complex using a spin polarized approach (U-B3LYP). The optimal geometry is almost identical to the experimental one: r(Ni–N) = 1.88 Å and θ = 58.0° (see Table 2). The binding energy after removal of BSSE, 0.48 eV, is slightly smaller than the experimental value, 0.57 eV. These results suggest that DFT describes the NO/Ni–MgO interaction in a satisfactory way. The binding of NO to Ni^{2+} is stronger than that of NO on low-coordinated Mg^{2+} ions [27], in agreement with the experimental findings. However, the analysis of the reference Kohn–Sham determinant shows an expectation value of the total spin operator, $\langle\hat{S}^2\rangle$, equal to 1.36, instead of 0.75 as expected for a pure doublet state. This indicates a large spin contamination by higher energy spin states due to the multiconfigurational character of the exact solution [11]. The Kohn–Sham determinant is characterized by three unpaired electrons, two with spin up mainly localized on the Ni atom, and one with spin down localized on the NO molecule. The resulting spin distribution is clearly in contrast with that deduced from EPR spectrum, which proves the presence of only one unpaired electron localized on the Ni atom 3d shell. The analysis of the spin density distribution and EPR properties is thus not possible at the U-B3LYP level [16].

For this reason the calculations have been repeated using the RO approach, which allows to produce pure spin states. The lowest state, $^2A''$, originates from the coupling of the unpaired electrons on the NO molecule and on Ni–MgO and correlates at infinite distance with NO^+ $^1\Sigma$ + $[NiMgO]^-$ $^2B_2$ (Ni^+ $3d^9$; $^2B_2$). The high spin $^4A''$ state, which correlates at infinite distance with NO $^2\Pi$ + NiMgO $^3B_2$ (Ni^{2+} $3d^8$; $^3B_2$), is purely repulsive [16]. The geometry optimization for the $^2A''$ state gives r(Ni–N) = 1.789 Å and θ = 60.5° (Table 2). Thus, also the spin restricted RO-B3LYP calculation leads to a geometry close to the experimental one.

So far the results of [16]. We present now an original discussion of the bonding based on the analysis of the molecular orbitals involved and of the dipole moment curve for the vertical motion of NO above the surface. On the (1 0 0) terraces of Ni–MgO the Ni^{2+} ions are in a C_{4v} symmetry. Coordination of NO lowers the symmetry to C_s, leading to Ni cations in a pseudo-octahedral coordination. The d_{z^2} and $d_{x^2-y^2}$ orbitals are destabilized by the interaction with the O^{2-} ligands, with the $d_{x^2-y^2}$ shifted to higher energies than the d_{z^2}. Coordination of NO does not cause any energy inversion among the d orbitals. The d_{z^2} orbital interacts strongly with the π^*_{xz} orbital of the NO molecule, forming a doubly occupied MO of A′ symmetry (Fig. 5a) confirming the high covalent character of the NO/Ni^{2+} interaction. One unpaired electron is left in the $d_{x^2-y^2}$ (A″) (Fig. 5b) in agreement with the EPR results. Finally, the LUMO (Fig. 5c) is the NO π^*_{xy} orbital which is not involved in the interaction with Ni^{2+}, being perpendicular to the d_{z^2} direction. This orbital is thus almost unperturbed by the presence of the oxide surface, and could be involved, at the most, in the back-donation from the filled Ni 3d orbitals normal to the *xy*-plane. The Ni^{2+} ion presents therefore a formal d^9 configuration (one hole in the d shell), although one of the electrons is shared with the NO molecule. The overall electron configuration of the system in the $^2A''$ state is thus $(d_{z^2} + \pi^*_{xz})^2(d_{x^2-y^2})^1(\pi^*_{xy})^0(d_{z^2} - \pi^*_{xz})$ O (d orbital index axis as in C_{4v} symmetry).

To show that the interaction of NO with the Ni^{2+} ion leads to the formation of a covalent bond, with virtually no electron transfer from the adsorbate to the substrate, we analyze the dipole moment curve [28,29]. The dipole moment of two point charges $+q$ and $-q$ is $\mu = -qz$; the first derivative is $d\mu/dz = -q$, assuming that $-q$ is at positive z with respect to $+q$. Hence, for an ideal fully ionic molecule where q = 1, $d\mu/dz = -1$ and the curve is a straight line. The Taylor expansion of the dipole moment curve about

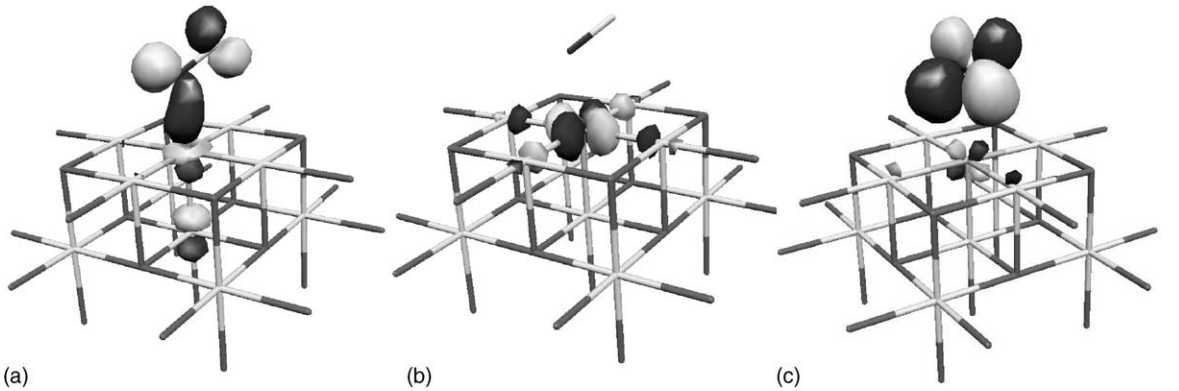

Fig. 5. Three-dimensional representation of relevant MO orbitals of NO/Ni–MgO system: (a) HOMO (A′), (b) SOMO (A″), (c) LUMO (A″).

the equilibrium $z = z_e$, is

$$\mu(z) = \mu_0 + \left(\frac{d\mu}{dz}\right)(z - z_e) + \left(\frac{d^2\mu}{dz^2}\right)(z - z_e)^2 \quad (1)$$

Therefore, while an ionic bond leads to a linear $\mu(z)$ with a large slope, a $\mu(z)$ curve with a small slope indicates that the bond is covalent [28,29]. In this study, the dipole moment curves, $\mu(z)$, of (i) a positive charge $+1$ on a $[NiMg_8O_9]^-$ bare cluster and (ii) the NO molecule on the $[NiMg_8O_9]$ cluster are plotted versus z, where z is the vertical distance from the oxide surface (Fig. 6). The positive charge is associated to an effective core potential in order to describe the finite dimension of an ion and to reduce the artificial polarization of the electron density; an electron has been added to Ni–MgO in the hypothesis that the Ni $3d^9$ ion has formed from a real charge transfer from the adsorbate. The dipole moment curve for the positive charge on a Ni^+ ion presents a large slope, $d\mu/dz = 1.22$, typical of ionic species. The slope is larger than 1 and the curve is not perfectly linear because of polarization effects [29]. On the contrary, in the case of the NO molecule the curve presents a very small slope, $d\mu/dz = -0.14$, as expected for a dominantly covalent bond.

Before we conclude this section, we comment on the ability of the spin restricted ROB3LYP method to reproduce the binding energy of NO to the Ni–MgO substrate [16]. The calculated D_e is 0.42 eV, but it reduces to -0.03 eV after BSSE correction (no binding) (Table 2). Therefore, the price to pay in order to have a correct spin eigenfunction is the loss of the interaction energy. This is due to the single determinant approach. Spin polarization introduced by performing UB3LYP calculations can approximately account for the configuration mixing which is required in order to describe this system (but completely fails in describing all spin related properties). Only explicitly correlated methods which account for the multireference character of the wavefunction are capable of producing a satisfactory description of all the properties of this system [16].

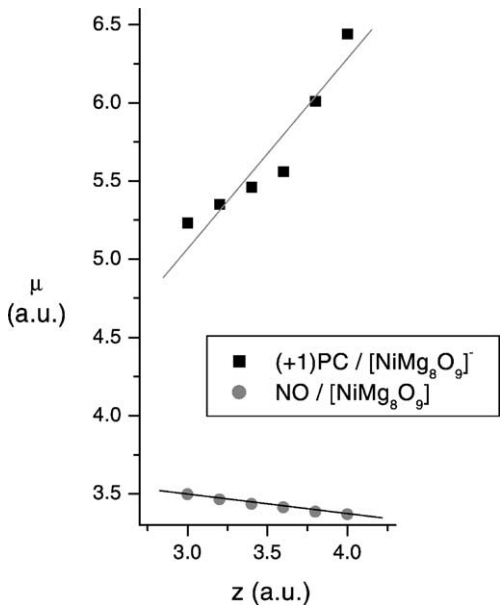

Fig. 6. Dipole moment curves for the RO-B3LYP solution of (i) a positive charge on $[NiMg_8O_9]^-$ and (ii) NO on $NiMg_8O_9$. The dipole moment $\mu(z)$ and the distance z are in a.u.

4. Conclusions

The EPR spectrum of NiO/MgO powders recorded at 77 K under NO pressure presents two clearly separated signals, assigned to monomeric NO adsorbed on low-coordinated Mg^{2+} ions (A signal) and to monomeric NO adsorbed on Ni^{2+} ions on terraces (B signal). In the presence of small amounts of Ni^{2+} in MgO matrix, the reactivity of the MgO surface is not altered with respect to the pure MgO high surface sample. Since at higher temperatures (RT) only signal B is observed, it is concluded that the binding energy of NO to Ni^{2+} is higher than with low-coordinated Mg^{2+} cations. Indeed, the calculated binding energy of NO on NiO(1 0 0) is about 0.5 eV, while NO is bound on low-coordinated cations of MgO by 0.1–0.2 eV only [27].

The EPR spectra show the presence of one unpaired electron localized on the Ni d shell. On the basis of RO-B3LYP calculations it is possible to assert that the unpaired electron in the Ni^{2+} d_{z^2} orbital couples with that in the NO π^*_{xz} orbital, forming a rather strong covalent bond. The second unpaired electron of Ni^{2+}, which gives rise to the EPR signal, sits on the $d_{x^2-y^2}$ orbital. The covalent character of the NO–Ni^{2+} bond is confirmed by the small slope of the dipole moment curve of the system with respect to the vertical distance of NO from the surface and by the analysis of the molecular orbitals. We conclude that, since there is no real net electron transfer from the NO molecule to the Ni^{2+} ion, the assignment of a "$3d^9$" configuration to the Ni atom in the NO/Ni–MgO system is only a formal representation of the resulting spin distribution.

Acknowledgements

This work has been supported by the PRA-ISADORA project of the Italian Istituto Nazionale per la Fisica della Materia (INFM) and by the Ministry of Education and University (MIUR) through a Cofin project.

References

[1] H.H. Kung, Transition Metal Oxides: Surface Chemistry and Catalysis, Elsevier, New York, 1989; J.N. Armor (Ed.), ACS Symp. Ser. 552 (1994).
[2] C. Xu, W.S. Oh, Q. Guo, D.W. Goodman, J. Vac. Sci. Technol. A 14 (1996) 1395.
[3] J.A. Rodriguez, T. Jirsak, M. Perez, L. Gonzales, A. Maiti, J. Chem. Phys. 114 (2001) 4186.
[4] A.P. Hagan, M.G. Lofthouse, F.S. Stone, M.A. Trevethan, in: B. Delmon, P. Grange, P. Jacob, G. Poncelet (Eds.), Preparation of Catalysts. II. Scientific Basis for the Preparation of Heterogeneous Catalysts, Elsevier, Amsterdam, 1979, p. 417.
[5] H.-J. Freund, Faraday Discuss. 114 (1999) 1.
[6] E.E. Platero, G. Spoto, A. Zecchina, J. Chem. Soc., Faraday Trans. 1 81 (1985) 1283.
[7] E.E. Platero, B. Fubini, A. Zecchina, Surf. Sci. 179 (1987) 404.
[8] E. Garrone, B. Fubini, E.E. Platero, A. Zecchina, Langmuir 5 (1989) 240.
[9] C. Xu, W.S. Oh, D.W. Goodman, J. Phys. Chem. 104 (2000) 10310.
[10] E. Giamello, E. Garrone, E. Guglielminotti, A. Zecchina, J. Mol. Catal. 24 (1984) 59.
[11] H. Kuhlenbeck, G. Odörfer, R. Jaeger, G. Illing, M. Menges, Th. Mull, H.-J. Freund, M. Pöhlchen, V. Staemmler, S. Witzel, C. Scharfschwerdt, K. Wennenmann, T. Liedtke, M. Neumann, Phys. Rev. B 43 (1991) 1969.
[12] R. Lindsay, P. Baumgartel, R. Terborg, O. Schaff, A.M. Bradshow, D.P. Woodruff, Surf. Sci. 425 (1999) L401.
[13] R. Wichtendahl, M. Rodriguez-Rodrigo, U. Härtel, H. Kuhlenbeck, H.-J. Freund, Surf. Sci. 423 (1999) 90.
[14] R. Wichtendahl, M. Rodriguez-Rodrigo, U. Härtel, H. Kuhlenbeck, H.-J. Freund, Phys. Status Sol. 173 (1999) 93.
[15] J.-T. Hoeft, M. Kittel, M. Polcik, S. Bao, R.L. Toomes, J.-H. Kang, D.P. Woodruff, M. Pascal, C.L.A. Lamont, Phys. Rev. Lett. 87 (2001) 086101-1.
[16] C. Di Valentin, G. Pacchioni, T. Bredow, D. Dominguez-Ariza, F. Illas, J. Chem. Phys. 107 (2002) 2299.
[17] M. Pöhlchen, V. Staemmler, J. Chem. Phys. 97 (1992) 2583.
[18] G. Pacchioni, A.M. Ferrari, A.M. Marquez, F. Illas, J. Comp. Chem. 18 (1997) 617.
[19] W.J. Stevens, H. Basch, M.J. Krauss, Chem. Phys. 81 (1984) 6026.
[20] T.R. Cundari, W.J. Stevens, J. Chem. Phys. 98 (1993) 5555.
[21] W.J. Hehre, R. Ditchfield, J.A. Pople, J. Chem. Phys. 56 (1972) 2257.
[22] V. Rassolov, J.A. Pople, M. Ratner, J.L. Windus, J. Chem. Phys. 109 (1998) 1223.
[23] A.D. Becke, J. Chem. Phys. 98 (1993) 5648.
[24] C. Lee, W. Yang, R.G. Parr, Phys. Rev. B 37 (1988) 785.
[25] S.F. Boys, F. Bernardi, Mol. Phys. 19 (1970) 553.
[26] M.J. Frisch, et al., Gaussian 98, Gaussian Inc., Pittsburgh, PA, 1997.
[27] C. Di Valentin, G. Pacchioni, M. Chiesa, E. Giamello, S. Abbet, U. Heiz, J. Phys. Chem. B 106 (2001) 1637.
[28] G. Pacchioni, P.S. Bagus, Surf. Sci. 286 (1993) 317.
[29] P.S. Bagus, G. Pacchioni, M.R. Philpott, J. Chem. Phys. 90 (1989) 4287.